

**Coherent vector meson photoproduction from deuterium at intermediate energies**T. C. Rogers,<sup>1</sup> M. M. Sargsian,<sup>2</sup> and M. I. Strikman<sup>1,\*</sup><sup>1</sup>*Department of Physics, Pennsylvania State University, University Park, Pennsylvania 16802, USA*<sup>2</sup>*Department of Physics, Florida International University, Miami, Florida 33199, USA*

(Received 16 January 2006; published 5 April 2006)

We analyze the cross section for vector meson photoproduction off a deuteron for the intermediate range of photon energies starting at a few giga-electron-volts above the threshold and higher. We reproduce the steps in the derivation of the conventional nonrelativistic Glauber expression based on an effective diagrammatic method while making corrections for Fermi motion and intermediate-energy kinematic effects. We show that, for intermediate-energy vector meson production, the usual Glauber factorization breaks down, and we derive corrections to the usual Glauber method to linear order in longitudinal nucleon momentum. The purpose of our analysis is to establish methods for probing interesting physics in the production mechanism for  $\phi$  mesons and heavier vector mesons. We demonstrate how neglecting the breakdown of Glauber factorization can lead to errors in measurements of basic cross sections extracted from nuclear data.

DOI: [10.1103/PhysRevC.73.045202](https://doi.org/10.1103/PhysRevC.73.045202)

PACS number(s): 11.80.Fv, 11.80.La

**I. INTRODUCTION**

Coherent vector meson production from nuclei has proven to be a useful tool for studying the structure of vector mesons. In the very high-energy, small-angle-scattering regime, well above the threshold for vector meson production, the large volume of available experimental data involving proton targets consistently supports the validity of the vector meson dominance (VMD) model for small photon virtualities [1,2]. This, combined with the onset of the eikonal regime in the diffractive region, has led to the development of a successful theoretical framework for the description of vector meson photoproduction off nuclei based on the combined VMD model and Glauber theory of hadron-nuclei rescattering [1,3]. The simplicity of the VMD-Glauber framework arises from the fact that at high energies the basic  $\gamma N \rightarrow VN$  and  $VN \rightarrow NN$  amplitudes vary slowly with the total energy of the  $\gamma N$  system relative to the range of important energies in the deuteron wave function. This observation leads to the factorizability of the basic  $\gamma N \rightarrow VN$  amplitude from the momentum space integral and yields the conventional Glauber multiple-scattering series consisting of nonrelativistic form factors and elementary scattering amplitudes.

The VMD-Glauber theory has led, in particular, to the demonstration that the coherent photoproduction of vector mesons off the deuteron at large  $-t$  is defined mainly by the rescattering contribution [4]. Since the  $VN \rightarrow VN$  amplitude appears in the double-scattering term, one may use nuclear photoproduction reactions to study the properties of vector mesons [5]. By choosing different  $t$ , one can control the relative distance at which rescattering may occur, which allows one to investigate the space-time evolution of hadronic systems produced in electro(photo)production.

The above program can be extended to the study of coherent vector electroproduction at large  $Q^2$ . In this case, coherent vector meson production from the deuteron can be

used to study color coherence/transparency phenomena in vector meson electroproduction at high  $Q^2$ . The onset of color transparency will reveal itself through the substantial drop in the double-scattering contribution with an increase of  $Q^2$  as opposed to the nearly energy-independent behavior of the double-scattering term for the generalized VMD prediction [5].

In this paper we consider yet another venue of application for vector meson photoproduction off nuclear targets by considering photoproduction in the intermediate range of energies starting a few giga-electron-volts above the threshold. These reactions have great potential for probing several effects such as non-diffractive mechanisms that violate the Okubo-Zweig-Iizuka (OZI) quark-line rule for vector meson production mesons, in-medium modifications of vector mesons, the importance of “nonideal”  $\omega - \phi$  mixing, and other new mechanisms for vector meson production (see Refs. [6–8]).

Finally, it would be interesting to learn whether the  $\phi$  meson is produced with a small enough transverse size that quark degrees of freedom may become relevant, as in the case of  $J/\psi$  production. Actually, in the case of  $J/\psi$ , the cross section of the  $J/\psi - N$  interaction  $\sigma_{J/\psi-N} \sim 3$  mb, [9] estimated based on the  $A$  dependence of  $J/\psi$  photoproduction at energies  $\sim 20$  GeV, is much larger than the estimate based on the VMD:  $\lesssim 1$  mb. This is likely due to the color transparency phenomenon [9]. A natural question is whether a trace of this effect remains in the case of  $\phi$  production. Jefferson Lab has produced data for  $\phi$  production that is currently being analyzed.

The interest in intermediate-energy reactions makes it necessary to reevaluate the assumptions of the traditional Glauber series method and to develop a new theoretical approach. This paper addresses the issues one must face when considering photon energies large enough that the eikonal approximation is an appropriate description of hadronic reinteractions, but not large enough that it is appropriate to neglect vector meson masses in kinematical calculations or any nontrivial  $s$  dependence of the amplitude for photoproduction of vector mesons from the nucleon. Furthermore, for small photon

\*Electronic address: [rogers@phys.psu.edu](mailto:rogers@phys.psu.edu)

energies ( $\lesssim 3$  GeV) the VMD hypothesis becomes suspect as a description of the  $\gamma N \rightarrow VN$  amplitude. Therefore we will not restrict ourselves to VMD model of  $\gamma N \rightarrow VN$  amplitude, considering instead the adequately parametrized form of photon-nucleon amplitudes. We argue in this paper that there may be a range of photon energies for which the eikonal approximation is valid, but in which the usual Glauber theory assumptions of factorization and ultrarelativistic kinematics break down.

Although we retain the eikonal approximation, our approach is distinctly different from the usual VMD-Glauber approach. In particular, one of the basic assumptions used in the Glauber approach is that the basic  $\gamma N \rightarrow VN$  and  $VN \rightarrow VN$  cross sections are slowly varying functions of center-of-mass energy and that the small Fermi momentum of the nucleons can be neglected in the evaluation of the total center-of-mass energy of the  $\gamma N$  and  $VN$  systems. These assumptions result in the usual factorizability already discussed above. At intermediate energies, however, the photon energy is comparable with the vector meson mass, and the basic amplitude may gain nontrivial energy dependence because Regge theory may be inadequate at intermediate photon energies. The usual smooth, slow rise in the total  $\gamma N \rightarrow VN$  cross section characteristic of high-energy diffractive scattering may be absent at intermediate energies. Fermi motion effects thereby destroy the factorizability of nuclear scattering into basic amplitudes and form factors. Also, the longitudinal momentum transferred (proportional to  $M_V^2/E_\gamma$ ) plays an important role as compared with reactions in the diffractive regime and further calls into question the factorization assumption. Earlier work (e.g., Ref. [10]) has considered the effect of longitudinal momentum transfers, but the breakdown of factorization has not been discussed.

To summarize, the particular reaction we are interested in in this paper is the coherent photoproduction of vector mesons from the deuteron. However, the energy dependence of the  $\gamma N \rightarrow VN$  will require that we account for Fermi motion effects that, in turn, will require that we account for nonfactorization effects. In the derivation of the total  $\gamma D \rightarrow VD$  amplitude we use the generalized eikonal approximation (GEA) with effective Feynman diagram rules (see, e.g., Refs. [11–14]). This is the approximation, valid at appropriately high energies, that allows us to derive the scattering amplitudes starting with corresponding effective Feynman diagrams while neglecting multiple scattering from the same nucleon. This is very similar to the GEA approach that has been applied to the  $A(e, e'p)X$  reactions on the nucleus [14].

By maintaining the result in terms of momentum space integrals, within the GEA, transferred longitudinal momentum and Fermi motion effects may be explicitly taken into account consistently. In our derivations, we keep only the corrections to the basic amplitudes that are of linear order in longitudinal exchanged momentum or nucleon momentum (neglecting order  $\mathbf{k}_N^2/m_N^2$  corrections, where  $\mathbf{k}_N$  is the bound-state nucleon momentum). This allows us to relate the  $D \rightarrow NN$  transition vertex to the nonrelativistic wave function of the deuteron. Since dynamical, model-dependent corrections related to the  $NN$  interaction are expected to be of quadratic or higher order in nucleon momentum, then linear-order corrections arising from

intermediate-energy kinematics should be taken into account *before* any specific theory of the basic bound-state amplitude that deviates from the nearly flat behavior of Regge theory is considered and used in the typical Glauber theory approach.

As explained above, we work in the kinematic regime in which diffractive behavior is not yet fully established but the momenta of the produced vector mesons are high enough that the eikonal approximation for the hadronic rescatterings is justified. As a result, a formalism should be maintained that allows the  $\gamma N \rightarrow VN$  and the  $VN \rightarrow VN$  amplitudes to be independently modeled. Fitting data to our modified form of the Glauber theory by using the  $VN \rightarrow VN$  amplitude as a parameter allows one to infer a value for the  $VN \rightarrow VN$  cross section. We emphasize that the main steps of this paper have been known for several decades; the Glauber theory in terms of effective Feynman diagrams was established in Ref. [11]. The effects of longitudinal momentum transfer in terms of phase shifts have also been studied [10]. However, as far as we are aware, there has never been direct numerical study of the effect of the breakdown of factorization in Glauber theory as it applies vector meson production. (The effects of factorization breakdown in proton knockout have been studied in Ref. [15].) One result that we find is that the breakdown of factorization persists even in the limit that off-shell effects in the bound-state nucleon amplitudes are negligible.

The paper is organized as follows: In Sec. II we derive scattering amplitudes for the  $\gamma D \rightarrow VD$  reaction based on the GEA. In Sec. III we discuss the steps needed to take into account linear-order corrections in nucleon momentum. In Sec. IV we perform a sample calculation in which we compare our results at intermediate-energy kinematics with the prediction of conventional VMD-Glauber theory. We identify the effects that are responsible for the divergence of the our approach from the standard Glauber theory. We demonstrate that effects calculated in this paper, if unaccounted for, can yield a misinterpretation of the  $VN$  scattering cross section if it is extracted from the data by use of the usual Glauber approximation. In a related issue, we discuss the recent data on  $\phi$  production at SPring-8/LEPS [16] and demonstrate the need to consider kinematic effects in the intermediate-energy region in Sec. V. In particular, these data suggest the importance of nonvacuum exchanges corresponding to  $\eta$  and  $\pi$  in the  $\phi$ -meson production mechanism at  $E_\gamma$  of a few giga-electronvolts. In Sec. VI we summarize our results. In Appendix A we describe the model of the basic amplitude that we used for our sample calculation, and in Appendix B we give an overview of the usual treatment of deuteron spin in Glauber theory.

## II. FORMULAS FOR THE AMPLITUDES

### A. Reaction and kinematics

We study the coherent photoproduction of vector mesons off the deuteron in the reaction

$$\gamma + D \rightarrow V + D', \quad (1)$$

where  $P \equiv (M_D, 0)$  and  $P' \equiv (E_D, \mathbf{P}')$  define the initial and final four-momenta of the deuteron. We use natural units ( $c = \hbar = 1$ ).  $q \equiv (E_\gamma, \mathbf{q})$  and  $P_V \equiv (E_V, \mathbf{P}_V)$  define the four-momenta of the initial photon and the final state meson

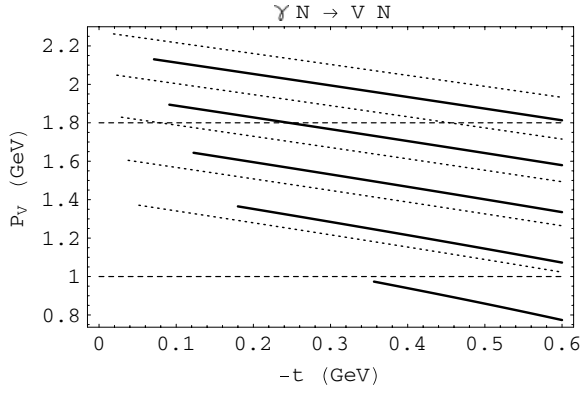


FIG. 1. Three-momentum of a vector meson produced by a photon scattering off a nucleon target as a function of  $-t$  for a given set of fixed  $E_\gamma$ . The solid lines correspond to  $\phi$ -meson production, whereas the dotted lines correspond to  $\rho^0$ -meson production. The incident photon energies in each case, going from the bottom curve to the top curve, are 1.6, 1.8, 2.0, 2.2, and 2.4 GeV. Details are discussed in the text.

respectively. The three-momentum transferred is defined as  $\mathbf{l} = \mathbf{q} - \mathbf{P}_V$ .

In our calculations we concentrate on *intermediate*-energy kinematics in which, although the photon energies are not high enough for the diffractive regime to be established for the photoproduction amplitude, the produced vector meson is sufficiently energetic that the eikonal approximation can be applied to the calculation of final-state hadronic rescatterings. This requires further elaboration: The GEA is the “straight-line” approximation in that the incident particle follows a nearly straight-line path through the nucleus. Clearly this must occur at high enough energies that higher partial waves than just the  $s$  wave contribute. To establish the appropriate kinematical regime for our approach, we have plotted in Fig. 1 the lab frame three-momentum of the final-state vector meson as a function of  $-t$  for a set of incident photon energies for the case of  $\rho^0$ - and  $\phi$ -meson production from a nucleon. Experience with the application of the Glauber model to the description of proton-nucleus scattering [17] as well as  $A(e, e'p)X$  reactions [18] indicates that the eikonal approximation works roughly for  $p_N/m_N \gtrsim 1$  ( $p_N$  is the proton three-momentum), and it works extremely well for  $E_N \gtrsim 2m_N$ . Since  $m_\phi \approx m_N$ , we expect to see the onset of the applicability of the GEA for a similar range of momenta for the case of  $\phi$ -meson production. By analogy with the proton case, we continue to use the criterion that  $E_\gamma \gtrsim 2M_V$ , and we find that the value of vector meson three-momentum above that the GEA may certainly be applied is  $P_V \gtrsim 1.8$  GeV for  $\phi$ -meson production. The values of three-momentum, 1 and 1.8 GeV, have been indicated by horizontal dashed lines in Fig. 1. These dashed lines in Fig. 1 may be viewed as separating kinematic configurations to which our approach may be applied to  $\phi$ -meson production from kinematic regions for which both the approach of this paper and the standard Glauber approach should be abandoned entirely with regards to  $\phi$ -meson production. Below  $P_V \approx 1$  GeV, both the approach of this paper and the usual Glauber approach should be abandoned. Between 1 and 1.8 GeV, the GEA

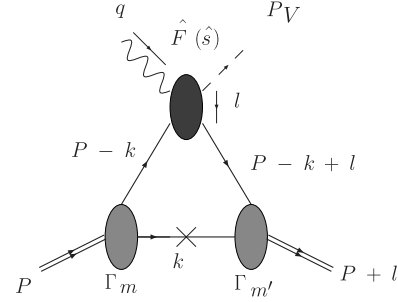


FIG. 2. The impulse diagram for photoproduction. The cross on the spectator nucleon line indicates that the spectator nucleon will be taken on-shell in the nonrelativistic approximation. (For all Feynman graphs we use Jaxodraw [19].)

may become a rough approximation, but above 1.8 GeV, the approach that we take in this paper by using the GEA is a very good approximation. For the  $\rho^0$  meson, the eikonal regime begins at smaller values of momentum than for the  $\phi$  meson because of its smaller mass, so to avoid confusion we do not include the corresponding range of applicability of the eikonal approach to  $\rho^0$ -meson production in Fig. 1.

Our main interest in this paper is the production of the  $\phi$  meson at around 3 GeV, so the application of the GEA is quite safe. We will find that another problem arises at  $t \approx t_{\min}$ , and this will be discussed in Sec. IV, but the above argument remains applicable as long as  $-t$  is more than a few tens of mega-electron-volts larger than  $-t_{\min}$ . We further assume that the nonrelativistic model of the  $NN$  interaction can be represented by a  $D \rightarrow NN$  vertex. In the case of the deuteron, there are only two relevant diagrams: the single-scattering diagram (Born term) of Fig. 2 and the double-scattering diagram of Fig. 3.

## B. The Born amplitude

We start with the calculation of the amplitude corresponding to the Born term of Fig. 2.  $F_{m,m'}^0(s, t)$  denotes the  $\gamma D \rightarrow VD$  scattering amplitude for the Born term in which only one of the nucleons takes part in the interaction, whereas  $\hat{F}(\hat{s}, t)$  denotes the basic  $\gamma N \rightarrow VN$  scattering amplitude. A hat on a variable indicates that it is associated with the  $\gamma N \rightarrow VN$  subprocess rather than the process of reaction (1). The superscript 0 is meant to distinguish the Born term from the double-scattering term. The initial and final polarizations of the deuteron are denoted by  $m$  and  $m'$ , respectively. Because we consider only

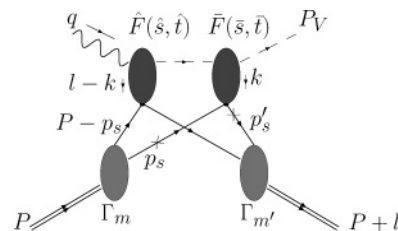


FIG. 3. The double-scattering diagram for photoproduction. The crosses on the spectator nucleon lines indicate that we will take poles corresponding to these nucleons going on-shell. (See Sec. II C.)

intermediate energies, the  $\hat{F}(\hat{s}, t)$  amplitude is not necessarily diffractive and we do not assume the validity of the VMD hypothesis. We neglect the spin-flip component of the basic amplitude (i.e.,  $\hat{F}$  and  $\bar{F}$  are approximately diagonal in nucleon spin). The  $D \rightarrow NN$  vertex is denoted by  $\Gamma_m$ . All variables correspond to the labels in the Feynman diagram of Fig. 2 for the single-scattering (Born) term. The free nucleon mass is denoted by  $m_N$ .

By applying effective Feynman rules to the graph in Fig. 2, we obtain the covariant scattering amplitude:

$$F_{m,m'}^0(s, t) = - \int \frac{d^4 \mathbf{k}}{i(2\pi)^4} \times \frac{\Gamma_{m'}^\dagger(P - k + l) \hat{F}(\hat{s}, t) \Gamma_m(P - k)}{[(P - k + l)^2 - m_N^2 + i\epsilon][(P - k)^2 - m_N^2 + i\epsilon][k^2 - m_N^2 + i\epsilon]} + (p \leftrightarrow n). \quad (2)$$

( $p \leftrightarrow n$ ) refers to the term in which the neutron and proton are inverted. In the remainder of this text, Mandelstam variables that appear within an integral are understood to be functions of internal nucleon four-momentum and the incident photon four-momentum.

We proceed with the derivation by estimating the loop integral in Eq. (2) up to terms of the order of  $\mathbf{k}^2/m_N^2$ . This approximation allows us to evaluate the integral in Eq. (2) by keeping only the pole contribution that yields a positive energy for the spectator nucleon. We find

$$F_{m,m'}^0(s, t) = \int \frac{d^3 \mathbf{k}}{(2\pi)^3} \times \frac{\Gamma_{m'}^\dagger(P - k + l) \hat{F}(\hat{s}, t) \Gamma_m(P - k)}{2k_0[(P - k + l)^2 - m_N^2 + i\epsilon][(P - k)^2 - m_N^2 + i\epsilon]} + (n \leftrightarrow p). \quad (3)$$

(Note that  $k_0 = m_N$  up to correction terms of the order of  $\mathbf{k}^2/m_N^2$ .) We now make use of the correspondence between the nonrelativistic wave function and the vertex function,

$$\tilde{\Psi}_m(\mathbf{k}_{\text{rel}}) \equiv \frac{-\Gamma_m(P - k)}{2\sqrt{k_0}(2\pi)^3 D(P - k)}, \quad (4)$$

the form of which is established by the Lippman-Schwinger equation [20] and by demanding that the nonrelativistic wavefunction be normalized to unity. Here,  $-D(P - k)$  is the propagator denominator of the struck nucleon. We write  $\mathbf{k}_{\text{rel}}$  to indicate that the argument of the wave function is the *relative* three-momentum of the two nucleons. Using Eq. (3) with Eq. (4) and using lab frame kinematics yields

$$F_{m,m'}^0(E_\gamma, l) = 2 \int d^3 \mathbf{k} \tilde{\Psi}_m^\dagger(\mathbf{k} - \mathbf{l}/2) \hat{F}(E_\gamma, k, l) \tilde{\Psi}_m(\mathbf{k}) + (n \leftrightarrow p). \quad (5)$$

We stress, at this point, that Eq. (5) does *not* yet coincide with the conventional VMD-Glauber theory because we have abandoned the usual assumptions that allow us to ignore the  $\mathbf{k}$  dependence in the basic amplitude, which would normally allow us to factor the basic amplitude out of the integral and leave us with the product of the basic amplitude with the nonrelativistic form factor. For heavier vector mesons (like the  $\phi$  meson), the vector meson mass may not be negligible, and the  $\hat{s}$  dependence of the basic amplitude becomes nontrivial at intermediate photon energies.

### C. The double-scattering amplitude

Having obtained the Born term in Eq. (3), we move on to calculate the double-scattering term of Fig. 3. Applying the effective Feynman diagrammatic rules, we obtain

$$F_{m,m'}^1(s, t) = - \int \frac{d^4 p_s}{i(2\pi)^4} \frac{d^4 p'_s}{i(2\pi)^4} \frac{\Gamma_m^\dagger(P + l - p'_s) \bar{F}(\bar{s}, \bar{t}) \hat{F}(\hat{s}, \hat{t}) \Gamma_m(P - p_s)}{[p_s^2 - m_N^2 + i\epsilon][p'_s{}^2 - m_N^2 + i\epsilon][(P - p_s)^2 - m_N^2 + i\epsilon]} \times \frac{1}{[(P + l - p'_s)^2 - m_N^2 + i\epsilon][(q - l + p'_s - p_s)^2 - M_V^2 + i\epsilon]} + (p \leftrightarrow n). \quad (6)$$

Figure 3 and Eq. (6) express the following sequence of events: The incident photon scatters from a nucleon with center-of-mass energy  $\sqrt{\hat{s}}$ , producing an intermediate state with invariant mass  $M_V$ . The intermediate state propagates through the deuteron before scattering from the other nucleon with center-of-mass energy  $\bar{s}$ . (Bars over variables indicate that they correspond to the secondary scattering.) We neglect fluctuations of the intermediate state for the present purposes. Now let us integrate over  $p_{s,0}$  and  $p'_{s,0}$ . The integration over  $p_{s,0}$  is similar to the integration over  $k_0$  for the Born term of Eq. (2). For the  $p'_{s,0}$  integration one can choose one of the positive-energy poles at  $M_D + l_0 - \sqrt{m_N^2 + (\mathbf{l} - \mathbf{p}'_s)^2} + i\epsilon$  and  $\sqrt{m_N^2 + \mathbf{p}'_s{}^2} - i\epsilon$  at the upper and lower complex semiplanes of  $p'_{s,0}$ . Note that within the approximation in which  $p_s'^2/m_N^2, l^2/m_N^2$  terms

are consistently neglected; the integration over either pole will yield the same result. We choose the  $\sqrt{m_N^2 + \mathbf{p}'_s{}^2} - i\epsilon$  pole (the poles chosen for integration are identified by the crosses shown in Fig. 3) because this choice reproduces the usual Glauber formula in the most direct way. Applying the definition in Eq. (4), we recover the formula quoted in [5]:

$$F_{m,m'}^1(E_\gamma, l) = - \int \frac{d^3 \mathbf{p}_s' d^3 \mathbf{p}_s}{(2\pi)^3} \times \frac{\tilde{\Psi}_m^\dagger(\frac{1}{2} - \mathbf{p}'_s) \bar{F}(\bar{s}, \bar{t}) \hat{F}(\hat{s}, \hat{t}) \tilde{\Psi}_m(-\mathbf{p}_s)}{\sqrt{p_{s,0} p'_{s,0}} [(q - l + p'_s - p_s)^2 - M_V^2 + i\epsilon]}. \quad (7)$$

The ( $p \rightarrow n$ ) term is implicit in these equations. Finally, we put this equation into a form that makes the next section slightly more manageable by transforming the variables of integration from  $p'_s$  and  $p_s$  to  $p \equiv (p_s + p'_s)/2$  and  $k \equiv p'_s - p_s$ , and we make the redefinitions  $k \rightarrow k + l/2$ , and  $p \rightarrow p + \frac{l}{4}$ . The result of these changes is

$$F_{m,m'}^1(E_\gamma, l) = - \int \frac{d^3\mathbf{p}d^3\mathbf{k}}{(2\pi)^3} \times \frac{\tilde{\Psi}_{m'}^\dagger(\mathbf{p} + \frac{\mathbf{k}}{2}) \bar{F}(\bar{s}, \bar{t}) \hat{F}(\hat{s}, \hat{t}) \tilde{\Psi}_m(\mathbf{p} - \frac{\mathbf{k}}{2})}{m_N [(q + k - \frac{l}{2})^2 - M_V^2 + i\epsilon]} + (p \leftrightarrow n). \quad (8)$$

In Eq. (8), we have given the amplitude a superscript, 1, to distinguish it from the Born term.

We summarize this section by cleaning up our notation and by writing out the correct expressions for the kinematic variables in terms of the integration variables, taking into account the variable transformations that were needed to get Eqs. (5) and (8). We explicitly expand each expression to linear order in nucleon momentum in the lab frame. Furthermore, we assume that nucleon three-momentum and the exchanged three-momentum are both small and of the same order of magnitude relative to all masses involved. Subscripts  $a$  denote Born amplitude quantities while subscripts  $b$  denote double-scattering quantities. The variables in each expression are established in the particular diagram under consideration. First, we have

$$\hat{s}_a = [(P - k) + q]^2 = m_N^2 + 2E_\gamma m_N + 2E_\gamma k_z + \mathcal{O}(\mathbf{k}^2). \quad (9)$$

Recalling the variable transformations we made in the double-scattering term and noting that  $\mathbf{p}$ ,  $\mathbf{k}$ , and  $\mathbf{l}$  are all of the same order of magnitude, we have

$$\hat{s}_b = (q + P - p_s)^2 = m_N^2 + 2E_\gamma m_N + 2E_\gamma \left( p_z - \frac{k_z}{2} \right) + \mathcal{O}(\mathbf{p}^2). \quad (10)$$

Note that there is only dependence on  $k_z$  and that  $\mathbf{k}$  contributions come into play only at higher order in nucleon momentum. For the rescattering amplitude, we get

$$\bar{s}_b = (k_V + p_s)^2 = M_V^2 + m_N^2 + 2E_V m_N - 2E_\gamma \left( p_z - \frac{k_z}{2} \right) + \mathcal{O}(\mathbf{p}^2). \quad (11)$$

This last value is obtained after the pole in  $k_z$  is taken, giving the intermediate state an invariant mass of  $k_V^2 = M_V^2$ . The values of  $t$  to be used in each of these cases is

$$\hat{t}_a = t \quad (12)$$

$$\hat{t}_b = \left( \frac{l}{2} - k \right)^2 = \left( \frac{l_0}{2} \right)^2 + \frac{l_z k_z}{2} - \left( \frac{l_\perp}{2} - k_\perp \right)^2 + \mathcal{O}(\mathbf{k}^2) \quad (13)$$

$$\bar{t}_b = \left( \frac{l}{2} + k \right)^2 = \left( \frac{l_0}{2} \right)^2 - \frac{l_z k_z}{2} - \left( \frac{l_\perp}{2} + k_\perp \right)^2 + \mathcal{O}(\mathbf{k}^2). \quad (14)$$

In the usual VMD-Glauber theory expression for the double-scattering term, one keeps only the perpendicular components of  $\hat{t}$  and  $\bar{t}$ . The terms proportional to  $k_z$  are small and, since they come with opposite sign, they tend to cancel if the  $t$  dependence of the basic amplitude is nearly exponential. The terms with  $l_0^2$  are proportional to  $t^2/M_D^2$ . Thus we continue to neglect both of the first two terms in Eqs. (13) and (14). Finally, we stress that  $(P - k)^2 = (M_D - m_N)^2 + \mathcal{O}(\mathbf{k}^2)$  so that the struck nucleon may be treated kinematically as being on-shell up to terms quadratic in the nucleon momentum.

By using the kinematic expressions of Eqs. (9)–(14) in Eqs. (5) and (8), we may ensure that the factors multiplying the deuteron wave function in each of the integrals is correct to linear order in nucleon three-momentum (or exchanged three-momentum).

### III. NUMERICAL ESTIMATES AND THE RELATIONSHIP WITH VMD-GLAUBER THEORY

#### A. Differential cross section

Now that we have calculated the Born and double-scattering amplitudes, let us set up notation that allows us to express the total differential cross section in terms of the basic amplitudes for  $\gamma N$  and  $VN$  scattering. We do not discuss any physics in this section, but simply formulate our notation to allow for convenient comparisons between the present approach and the standard VMD-Glauber approach.

For any exclusive two-body reaction involving incoming particles of masses  $m_1$  and  $m_2$  and center-of-mass energy squared  $s$ , the differential cross section may be represented as follows:

$$\frac{d\sigma^{m,m'}}{dt} = \frac{1}{16\pi \Phi(s, m_1, m_2)} |F_{m,m'}(s, t)|^2, \quad (15)$$

where

$$\Phi(s, m_1, m_2) \equiv [(s - m_1^2)^2 + m_2^4 - 2sm_2^2 - 2m_1^2m_2^2]. \quad (16)$$

In particular, the differential cross section for reaction (1) is

$$\frac{d\sigma^{m,m'}}{dt} = \frac{1}{16\pi \Phi(s, 0, m_N)} |F_{m,m'}^0(s, t) + F_{m,m'}^1(s, t)|^2. \quad (17)$$

It follows from Eqs. (2) and (8) that the numerical calculations of Eq. (17) will require as input the amplitudes for for both the  $\gamma N \rightarrow VN$  and the  $VN \rightarrow VN$  interactions.

To proceed, we construct a parametrization of the photo-production differential cross section in a form that will provide a smooth transition to the VMD-Glauber regime by writing

$$\frac{d\hat{\sigma}^{\gamma N \rightarrow VN}}{dt}(\hat{s}, \hat{t}) = \frac{\hat{n}_0^2}{16\pi} \left( \frac{\hat{s}}{\hat{s}_0} \right)^{2(\hat{\alpha}(\hat{t})-1)} \hat{f}^2(\hat{t}) \hat{g}^2(\hat{s}, \hat{t}) \quad (18)$$

for the basic  $\gamma N \rightarrow VN$  interaction. In the high-energy photon limit, the function  $\hat{f}(\hat{t})$  reduces, by construction, to the usual exponential dependence  $e^{\hat{B}\hat{t}/2}$ , with the constant  $\hat{B}$  that is typically used to parametrize experimental data as in, for example, Ref. [1]. The Regge trajectory is  $\hat{\alpha}(t) = \hat{\alpha}'t + \hat{\alpha}_0$ . The factor of  $(s/s_0)^{\hat{\alpha}(\hat{t})-1}$  is the Regge parametrization obtained in the VMD-Glauber regime, and  $\hat{g}(\hat{s}, \hat{t})$  is a function that adjusts for other  $s$  and  $t$  dependences that may appear in the

intermediate-energy regime, but such that  $\hat{g}(\hat{s}, 0)(s/s_0)^{\hat{\alpha}(0)-1}$  reduces to 1 in the high-energy photon limit. By substituting Eq. (18) into Eq. (15), we obtain

$$\hat{F}^{\gamma N \rightarrow VN}(\hat{s}, \hat{t}) = \hat{n}_0(\hat{s} - m_N^2) \left( \frac{\hat{s}}{\hat{s}_0} \right)^{\hat{\alpha}(\hat{t})-1} \hat{f}(\hat{t}) \hat{g}(\hat{s}, \hat{t})(i + \hat{\eta}). \quad (19)$$

The overall normalization is labeled  $\hat{n}_0$  and is not necessarily related to a total cross section. The variable  $\hat{\eta}$  is a possible real contribution to the amplitude. Because  $P_V \gtrsim 1$  GeV for the kinematic regime under consideration (see Sec. II A), the parametrization we use for the  $VN \rightarrow VN$  simply takes a nearly diffractive form:

$$\bar{F}^{VN \rightarrow VN}(\bar{s}, \bar{t}) = \sigma_{VN}(\bar{s})(i + \bar{\eta}) \sqrt{\Phi(\bar{s}, m_N, M_V)} \bar{f}(\bar{s}, \bar{t}). \quad (20)$$

The function  $\bar{f}(\bar{s}, \bar{t})$  reduces by construction to a Regge parametrization,  $(\bar{s}/\bar{s}_0)^{\bar{\alpha}(\bar{t})-\bar{\alpha}(0)} e^{\bar{B}\bar{t}/2}$  in the VMD regime. By applying the optical theorem to Eq. (20), we see that  $\sigma_{VN}(\bar{s})$  is, indeed, the total  $VN$  cross section. The variable  $\bar{\eta}$  is a possible real part of the amplitude.

Our peculiar choice of notation is made so that we may smoothly recover the usual Regge parametrizations when we consider the VMD-Glauber approximation. Indeed, applying the VMD hypothesis in the appropriate kinematical regime allows us to assume that  $\hat{F}(\hat{s}, \hat{t}) \propto \bar{F}(\bar{s}, \bar{t})$ . Thus applying the optical theorem would allow one to deduce the  $VN \rightarrow VN$  amplitude. With the standard high-energy approximations, we have

$$\begin{aligned} \hat{F}(\hat{s}, \hat{t}) &\xrightarrow{E_\gamma \gg M_V} \hat{s} \hat{n}_0 (i + \hat{\eta}) \hat{s}^{\hat{\alpha}'\hat{t}} e^{\hat{B}\hat{t}/2}, \\ \bar{F}(\bar{s}, \bar{t}) &\xrightarrow{E_\gamma \gg M_V} \bar{s} \sigma_{VN} (i + \bar{\eta}) \bar{s}^{\bar{\alpha}'\bar{t}} e^{\bar{B}\bar{t}/2}. \end{aligned} \quad (21)$$

Here we have put  $\hat{s}_0 = 1$  GeV for convenience as is often done in parametrizations. In this way, we show how our parametrizations reduce smoothly to the expressions obtained within Regge theory and the VMD hypothesis.

One may fit all of the functions that define the expression for  $\hat{F}(\hat{s}, \hat{t})$  directly to data for  $[(d\sigma^{\gamma N \rightarrow VN})/dt]$ . The function  $\hat{g}(\hat{s}, \hat{t})$  has been introduced to account for peaks in the energy dependence or other irregular energy dependence at intermediate energies. Without the VMD hypothesis, we can assume no relationship between  $\hat{F}(\hat{s}, \hat{t})$  and  $\bar{F}(\bar{s}, \bar{t})$ . At intermediate energies, therefore,  $\bar{F}(\bar{s}, \bar{t})$  must be obtained from a theoretical model or by other experimental means. Conversely, one can use data for reaction (1) to extract  $\bar{F}(\bar{s}, \bar{t})$ .

## B. Corrections to factorizability and an effective form factor

We now define an effective form factor

$$\begin{aligned} S_{\text{eff}}^{m,m'} \left( E_\gamma, \frac{\mathbf{l}}{2} \right) &\equiv \int \frac{d^3\mathbf{k}(\hat{s}_a - m_N^2)}{2E_\gamma m_N} \left( \frac{\hat{s}_a}{2E_\gamma m_N} \right)^{\alpha(\hat{t})-1} \\ &\times \hat{g}(\hat{s}, \hat{t}) \tilde{\Psi}_{m'}^\dagger \left( \mathbf{k} - \frac{\ell}{2} \right) \tilde{\Psi}_m(\mathbf{k}) \end{aligned} \quad (22)$$

for the Born term, and an effective basic amplitude

$$\hat{F}_{\text{eff}}^0(E_\gamma, t) \equiv 2E_\gamma m_N \hat{n}_0 (i + \hat{\eta}) \left( \frac{2E_\gamma m_N}{s_0} \right)^{\alpha(\hat{t})-1} f(t). \quad (23)$$

If we substitute Eq. (19) into Eq. (5), then the Born amplitude for production from the deuteron is

$$F_{m,m'}^0(E_\gamma, l) = 2\hat{F}_{\text{eff}}^0(E_\gamma, l) S_{\text{eff},a}^{m,m'}(E_\gamma, l/2) + (n \leftrightarrow p). \quad (24)$$

The definition in Eq. (23) takes the form of a general diffractive parametrization obtained when one makes the VMD hypothesis. However, Eq. (24) is exactly correct without any approximations. We have recovered the usual structure of the Born expression—the product of a diffractive basic amplitude with a form factor. The new feature in Eq. (24) is that our effective form factor depends on the energy of the photon. The definitions that we made in Eqs. (22) and (23) ensure that the effective form factor and the effective diffractive amplitude reduce to the usual nonrelativistic form factor and the true diffractive basic amplitude in the limit that  $E_\gamma \gg M_V$ :

$$\begin{aligned} S_{\text{eff}}^{m,m'}(E_\gamma, \ell/2) &\xrightarrow{E_\gamma \gg M_V} S_{\text{eff}}^{m,m'}(\ell/2), \\ \hat{F}_{\text{eff}}^0(E_\gamma, l) &\xrightarrow{E_\gamma \gg M_V} \hat{F}^{VN \rightarrow VN}(\hat{s}, t). \end{aligned} \quad (25)$$

By following the usual methods of VMD-Glauber theory, one will extract the *effective* amplitude from the  $\gamma D \rightarrow VD$  cross section rather than the true amplitude. If, in the region of very small  $-t$ , where the Born cross section dominates, the amplitude for the  $\gamma N \rightarrow VN$  scattering is inferred from data by use of the usual VMD-Glauber theory, then Eq. (24) can be used to obtain a corrected amplitude that accounts for nonfactorizability.

## C. Corrections to factorizability in double scattering

The double-scattering term is more complicated because, in Eq. (8), the energy dependence cannot easily be factorized out of the integrand. We may rewrite Eq. (8) by using Eqs. (19) and (20) as

$$\begin{aligned} F_{m,m'}^1(E_\gamma, t) &= - \int dk_z \int d^2\mathbf{k}_\perp \int \frac{d^3\mathbf{p}}{(2\pi)^3} \\ &\times \frac{\hat{f}(\hat{t}_b) \bar{f}(\bar{s}_b, \bar{t}_b) \tilde{\Psi}_{m'}^\dagger(\mathbf{p} + \frac{\mathbf{k}}{2}) \tilde{\Psi}_m(\mathbf{p} - \frac{\mathbf{k}}{2})}{m_N [(q + k - \frac{l}{2})^2 - M_V^2 + i\epsilon]} \\ &\times \left[ \left( \frac{\hat{s}}{s_0} \right)^{\hat{\alpha}(\hat{t})-1} \sqrt{\Phi(\hat{s}, m_N, 0) \Phi(\bar{s}, m_N, M_V)} \right] \\ &\times \hat{g}(\hat{s}, \hat{t}) \hat{n}_0 \sigma_{VN}(\bar{s}) (i + \hat{\eta}) (i + \bar{\eta}). \end{aligned} \quad (26)$$

The nonfactorizability of Eq. (26) near threshold comes from the fact that the basic amplitudes and the factors in braces have nontrivial dependence on the integration variables. We determine that there is no simple reformulation of the integral in Eq. (26) that consistently accounts for corrections linear in momentum. Therefore we conclude that a direct numerical evaluation is necessary. Note that, although we have set up the integral for a specific parametrization, the analysis applies to any smooth, slowly varying energy-dependent basic amplitude. One determines  $k_z$  integral by expanding the

denominator in Eq. (26):

$$\begin{aligned} & \left(q + k - \frac{l}{2}\right)^2 - M_V^2 + i\epsilon \\ & \approx 2E_\gamma \left[-k_z + \frac{l_z}{2} - \frac{M_V^2}{2E_\gamma} + \left(k - \frac{l}{2}\right)_0 + i\epsilon\right] \\ & = 2E_\gamma[-k_z - \Delta + i\epsilon]. \end{aligned} \quad (27)$$

The second line fixes the definition of  $\Delta$ . Note that, by ignoring the term  $(k - \frac{l}{2})^2/2E_\gamma$ , we have ignored the possibility of contributions from intermediate mesons that are far off-shell and that correspond to nucleon three-momenta that are strongly suppressed by the deuteron wave function. Furthermore, note that the pole value of  $k_z$  in this approximation depends on only the external variables and is independent of the transverse motion of the nucleons. The resulting double-scattering amplitude is then

$$\begin{aligned} F_{m,m'}^1(E_\gamma, t) &= \int d^2\mathbf{k}_\perp \int \frac{d^3\mathbf{p}}{(2\pi)^2} \int_{-\infty}^{\infty} \frac{dk_z}{(2\pi)} \\ & \times \frac{\hat{f}(\hat{t}_b) \bar{f}(\bar{s}_b, \bar{t}_b) \tilde{\Psi}_{m'}^\dagger(\mathbf{p} + \frac{\mathbf{k}}{2}) \tilde{\Psi}_m(\mathbf{p} - \frac{\mathbf{k}}{2})}{2E_\gamma m_N [k_z + \Delta - i\epsilon]} \\ & \times \left(\frac{\hat{s}}{s_0}\right)^{\hat{\alpha}(\hat{t})-1} \sqrt{\Phi(\hat{s}, m_N, 0) \Phi(\bar{s}, m_N, M_V)} \\ & \times \hat{g}(\hat{s}, \hat{t}) \hat{n}_0 \sigma_{VN}(\bar{s}_b) (i + \hat{\eta})(i + \bar{\eta}) \\ & \equiv \int d^2\mathbf{k}_\perp \int \frac{d^3\mathbf{p}}{(2\pi)^2} \\ & \times \int_{-\infty}^{\infty} \frac{dk_z}{(2\pi)} \frac{I_{m,m'}(\mathbf{k}_\perp, k_z, \mathbf{p}, s)}{2E_\gamma m_N [k_z + \Delta - i\epsilon]}. \end{aligned} \quad (28)$$

We have gathered all factors apart from the energy denominators in the integrand into a function  $I_{m,m'}(\mathbf{k}_\perp, k_z, \mathbf{p}, s)$ . Assuming identical protons and neutrons, we get an identical term for the case in which the roles of the neutron and proton are inverted. A convenient way to reorganize this formula so that it more closely resembles the nonrelativistic quantum-mechanical theory is to write the integrand in terms of its Fourier components in the following mixed representation:

$$I_{m,m'}(k_\perp, k_z, \mathbf{p}, s) = \frac{1}{\sqrt{2\pi}} \int_{-\infty}^{\infty} dz \tilde{I}_{m,m'}(\mathbf{k}_\perp, z, \mathbf{p}, E_\gamma) e^{-ik_z z}. \quad (29)$$

The vector meson propagator may be rewritten with the identity

$$\frac{1}{p - i\epsilon} = \int_{-\infty}^{\infty} dz \Theta(-z) e^{i(p-i\epsilon)z}. \quad (30)$$

Summing the two terms for the neutron and the proton and using the fact that  $\Theta(z) + \Theta(-z) = 1$  yields

$$\begin{aligned} F_{m,m'}^1(E_\gamma, t) &= i \int \frac{d^3\mathbf{p} d^2\mathbf{k}_\perp}{2E_\gamma m_N (2\pi)^2} I_{m,m'}(\mathbf{k}_\perp, -\Delta, \mathbf{p}, E_\gamma) \\ & - \frac{1}{\sqrt{2\pi}} \int \frac{d^3\mathbf{p} d^2\mathbf{k}_\perp}{2E_\gamma m_N (2\pi)^2} \\ & \times \int_{-\infty}^{\infty} dz \tilde{I}_{m,m'}(\mathbf{k}_\perp, z, \mathbf{p}, s) \sin(-\Delta z) \Theta(z). \end{aligned} \quad (31)$$

In the VMD-Glauber approximation,  $\Delta \rightarrow 0$ , and  $I_{m,m'}(\mathbf{k}_\perp, 0, \mathbf{p}, s)$  is the usual energy-independent density matrix. Hence the first term in Eq. (31) reduces to the traditional Glauber expression for double scattering, and the second term vanishes in the limit for which the usual VMD-Glauber assumptions are applicable. The second term is a correction, discussed in Ref. [5], that arises from the nonzero phase-shift in the vector meson wave function induced by longitudinal momentum transfer. In the phase-shift term, the factor of  $\sin(-\Delta z)$  is itself a correction of the order of  $k_z$ , so we neglect Fermi motion and energy-dependent corrections to  $I_{m,m'}(\mathbf{k}_\perp, 0, \mathbf{p}, s)$  in the phase-shift term.

For a real photon, the double-scattering term picks out the relative longitudinal nucleon momentum:

$$\Delta = \frac{l_-}{2} + \frac{M_V^2}{2E_\gamma}. \quad (32)$$

Furthermore,  $l_- = -(M_V^2 - t)/2E_\gamma$ , so

$$\Delta = \frac{t + M_V^2}{4E_\gamma}, \quad (33)$$

and we see that  $\Delta$  is indeed negligible at large center-of-mass energies and small  $t$ . Corrections to the double-scattering term, at linear order in momentum, arise from performing the integral in the first term of Eq. (31) numerically and by retaining the phase-shift term. We end this section by noting that the breakdown in factorization comes simultaneously from the fact that longitudinal momentum transfer is nonnegligible and the fact that the longitudinal momentum of the bound nucleons is nonnegligible; the contribution to the basic amplitudes from the longitudinal component of the bound nucleon momentum at linear order would vanish by symmetry in all of the integrals if the longitudinal momentum transfer were neglected in the wave functions.

## IV. SAMPLE CALCULATIONS

### A. Cross-section calculation

It is usually the case that one calculates the charge and quadrupole form factors in the coordinate space formulation of the form factor. This method reduces the formulas to an extremely simple form and allows one to deal simply and directly with polarizations. For the purpose of modifying the basic amplitude, however, so that it has nucleon momentum dependence, we must maintain the momentum space formulation that results from a direct evaluation of the effective Feynman diagrams in Figs. 2 and 3. Carrying this procedure out was the topic of the previous two sections. The calculation is straightforward, but becomes numerically cumbersome, and the longitudinal momentum exchanged leads to a breakdown of the orthogonality relations for spherical harmonics that usually lead to a very simple coordinate space formulation. However, dealing with the deuteron polarizations can still be simplified if one chooses the axis of quantization along the direction of momentum exchange [3,21]. An overview of the nonrelativistic deuteron wave function with polarizations is given in Appendix B.

In this section we provide some sample calculations by using simple models of the basic amplitudes. To this end, we restore the assumption of VMD and we use very simple parametrizations of the  $s$  and  $t$  dependences in the basic amplitudes. The purpose for doing this is mainly to provide estimates of the sensitivity to nonfactorizability rather than because VMD is thought to be appropriate at intermediate energies. We extracted estimates of the parameters for production of the  $\rho^0$  and  $\phi$  vector mesons from the basic nucleon interaction cross-section data appearing in Ref. [1], and we made rough estimates of the parametrization of the  $s$  and  $t$  dependences of these amplitudes (see Appendix A for a description of our parametrizations). This provides us with a reasonable model to work with, though we stress that refinements are ultimately needed. For all of our calculations we use the nonrelativistic wave function obtained from the Paris  $NN$  potential [22].

We are mainly interested in the  $\phi$ -production cross section that is dominated by natural parity exchange, even at energies close to threshold, because of the OZI rule. However, to demonstrate the consistency of our approach with traditional methods, we consider first the case of the photoproduction of  $\rho^0$  mesons, which has been well understood for some time. The basic amplitude for  $\rho^0$  production is dominated by soft Pomeron exchange at large energies, so that it is constant at high energies, but undergoes a relatively steep rise at energies near threshold because of meson exchanges. The parametrization we use is shown in appendix A. We use a typical exponential slope factor of  $7.0 \text{ GeV}^{-2}$  for the  $t$  dependence. Figure 4 shows the cross section for  $\rho^0$  production at the high energy of  $E_\gamma = 12.0 \text{ GeV}$ . For comparison, we show data taken at  $12.0 \text{ GeV}$  from Refs. [1,4]. The comparison with data is reasonable, as it is with the traditional Glauber approach.

Now we consider the more interesting case of  $\phi$ -meson photoproduction. At high energy, we use the Regge dependence,  $\alpha(t) = 0.27t + 1.14$  given in Ref. [1]. The parametrization that we used is described further in Appendix A. As noted in Ref. [1], the energy dependence of the  $\phi$ -meson photoproduction cross section is very weak, but the current state of experimental data is still ambiguous as to how much this energy dependence continues at lower energies. However, the large negative ratio of the real to imaginary part of the

amplitude ( $\eta = -0.48$ ) [23] suggests that some mechanism other than soft Pomeron exchange is significant. This value of the ratio of the real to imaginary part of the  $\phi$ -meson cross section has large error bars and was calculated with the longitudinal momentum transfer neglected. However, it is the only measurement we know of at the moment so we use it for the purpose of demonstration. At lower photon energies than what we consider here, the energy dependence of the basic cross section may become highly nontrivial as is suggested by data in Ref. [16]. The results of the calculation done with each combination of initial and final deuteron polarizations are shown in the separate panels for a photon energy of  $E_\gamma = 30.0 \text{ GeV}$  in Fig. 5 and for a photon energy of  $E_\gamma = 3.0 \text{ GeV}$  in Fig. 6. The result is summarized in Figs. 7 and 8, which show the differential cross section for different polarizations along with the unpolarized cross section for photon energies of  $30.0$  and  $3.0 \text{ GeV}$ , respectively.

Each of the curves in Figs. 5 and 6 separately represents the contribution to the total cross section from a term in the squared amplitude when we apply Eq. (17). The Born and double scattering terms are obtained from the square of Eq. (24) and square of the first term of Eq. (31), respectively. The phase-shift term arises from the square of the second term in Eq. (31). We call it the phase-shift term because, in the language of nonrelativistic quantum-mechanical wave functions, it arises because of a phase difference between the incoming photon and the produced vector meson. The interference term arises from the interference between Eqs. (24) and (31). Note that the interference term is negative, but it is plotted on the positive axis for demonstration purposes. Note also that there is no contribution from the Born term for the  $m = +/ - 1$  to  $m = -/ + 1$  transition, and therefore the total cross section for the spin-flip reaction has none of the large dips characteristic of the Born cross section.

An important feature that can be seen in Figs. 5 and 6 is that the double-scattering term is suppressed in the intermediate-energy case relative to the high-energy case. We can see this most clearly by comparing the upper left-hand panel of Fig. 5 with the upper left-hand panel of Fig. 6. It is clear that the double-scattering contribution is important in the  $E_\gamma = 30 \text{ GeV}$  case at moderate values of  $-t$ , whereas for the  $E_\gamma = 3 \text{ GeV}$  case the cross section is dominated by the Born term all the way up to  $-t \approx 0.4 \text{ GeV}^2$ . In the general case of multiple scattering from complex nuclei, it is the rescattering contributions that lead to the usual  $A$  dependence ( $A$  is the number of nucleons) of Glauber theory. The fact that multiple scattering is suppressed in double scattering in the deuteron suggests that our method would yield a rather different  $A$  dependence from that of usual Glauber theory if it were extended to complex nuclei. Extending our approach to complex nuclei will be the subject of future work.

Another problem begins to emerge at lower photon energies and extremely small  $-t$  (at  $t \approx t_{\min}$ ): A large fraction of the momentum integrals begins to violate relativistic kinematic constraints. It is likely that the basic amplitudes vary extremely rapidly with  $s$  and  $-t$  in these regions of the integral and that expanding in nucleon momentum is not valid (at least to linear order). To make progress, a precise understanding of the dynamics of off-shell amplitudes based on field theory

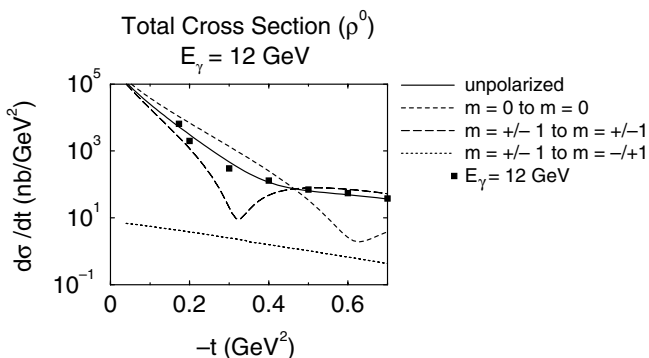


FIG. 4. The unpolarized differential cross section for coherent  $\rho^0$ -meson production compared with the total cross section for different polarizations. The calculation is done with the large photon energy  $E_\gamma = 12 \text{ GeV}$ , and the data for  $E_\gamma = 12 \text{ GeV}$  are taken from Ref. [1].



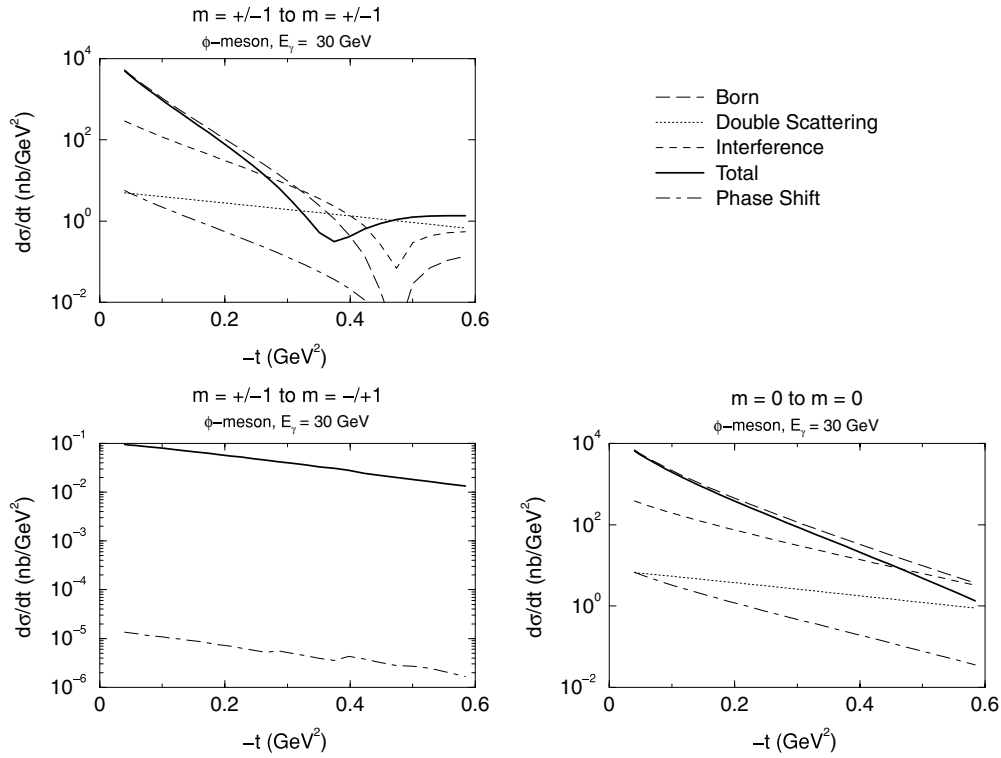


FIG. 5. The long-dashed, dotted, dashed, solid, and dot-dashed lines refer to the Born, double, interference, total, and phase-shift terms, respectively, for a photon energy of  $E_\gamma = 30.0$  GeV. The interference term is negative but is plotted for illustration on the positive axis. See text for detailed discussion.

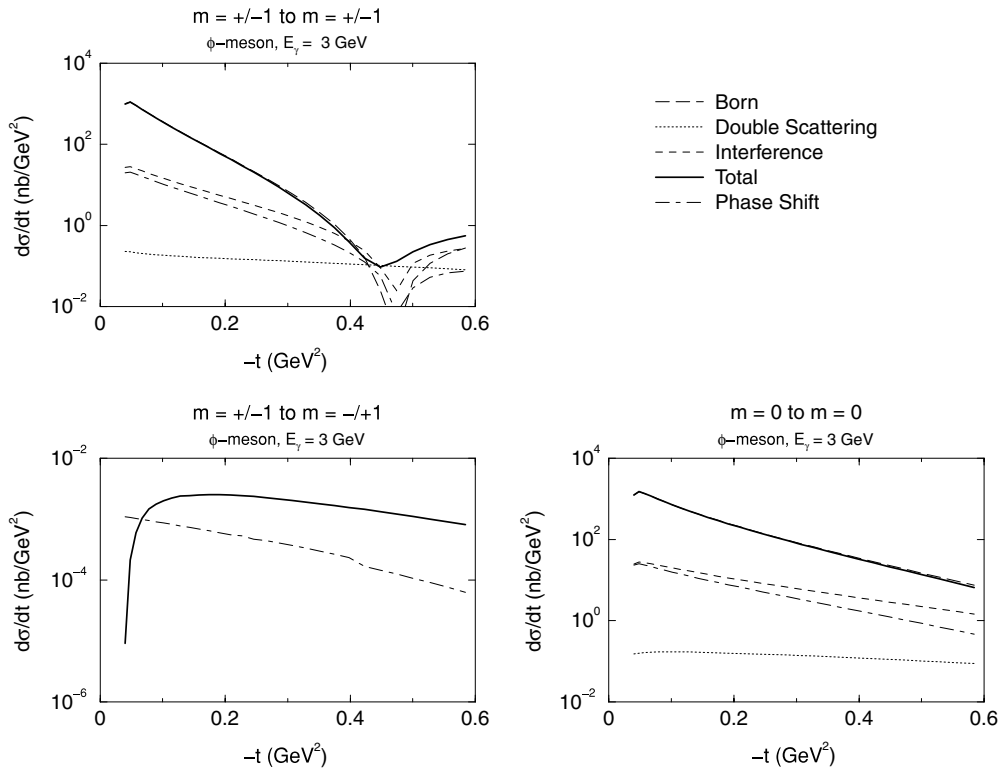


FIG. 6. The long-dashed, dotted, dashed, solid, and dot-dashed lines refer to the Born, double, interference, total, and phase-shift terms, respectively, for a photon energy of  $E_\gamma = 3.0$  GeV. Note the different scale on the axis for the spin-flip contribution. The interference term is negative but is plotted for illustration on the positive axis. See text for detailed discussion.

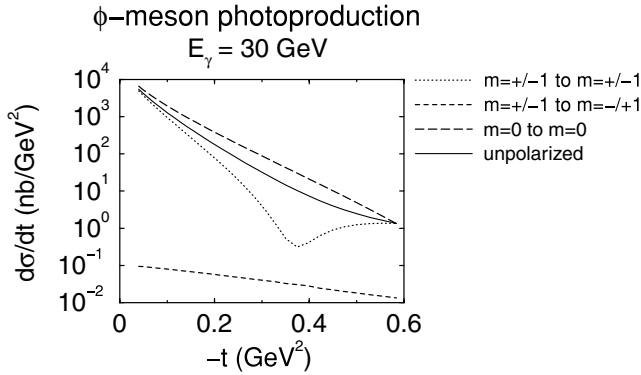


FIG. 7. The differential cross section for  $\phi$ -meson production for different polarizations for a photon energy of  $E_\gamma = 30.0$  GeV. See text for detailed discussion.

may be necessary. Therefore our approximation is valid only at  $-t$  sufficiently large that the integrand does not contain significant contributions from kinematically forbidden nucleon configurations. We tested the effect of this region in our calculations, and in performing our calculation, we found that there is virtually no contribution from kinematically forbidden regions for any situation that we consider as long as  $-\hat{t} + \hat{t}_{\min}$  is greater than a few tens of mega-electron-volts. We note that, even at relatively low photon energies, the data are consistent with a smooth exponential  $-t$  dependence (see Ref. [16]) as long as  $-t$  is not exactly  $-t_{\min}$ . Note that this theoretical problem of considering  $t$  at exactly  $-t_{\min}$  exists at high energies as well, but that at high energies  $-t_{\min}$  is generally too small for it to show up in plots. So that we may perform our calculations numerically at all values of  $-t$  greater than  $-t_{\min}$ , we choose to make the basic amplitude vanish in kinematically forbidden configurations (when  $-t \leq -\hat{t}_{\min}$ ). This results in a small dip just above  $-t_{\min}$  in our plots. The small dip is therefore unphysical, and should not be regarded as a prediction. We leave it in our plots merely to illustrate a general failure of the Glauber theory approach at extremely small  $-t$  (see Fig. 8 at  $-t \lesssim 0.06$  GeV<sup>2</sup>). In summary of the above, the small dip at extremely small  $-t$  denotes

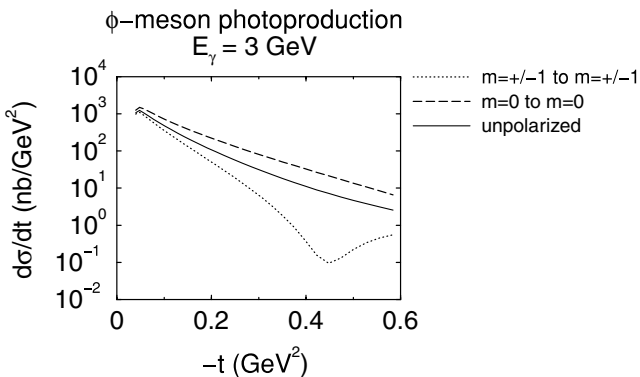


FIG. 8. The differential cross section for  $\phi$ -meson production for different polarizations for a photon energy of  $E_\gamma = 3.0$  GeV. The deuteron spin-flip term is negligible at these energies. See text for detailed discussion.

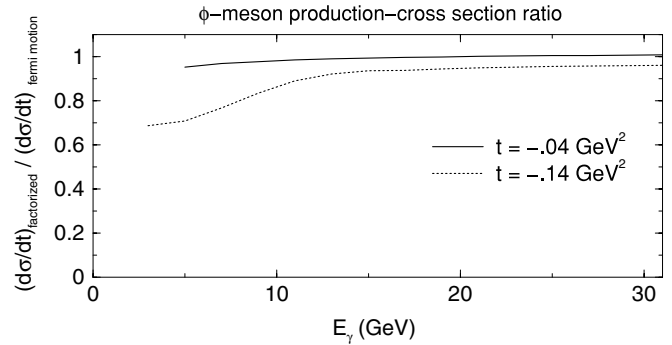
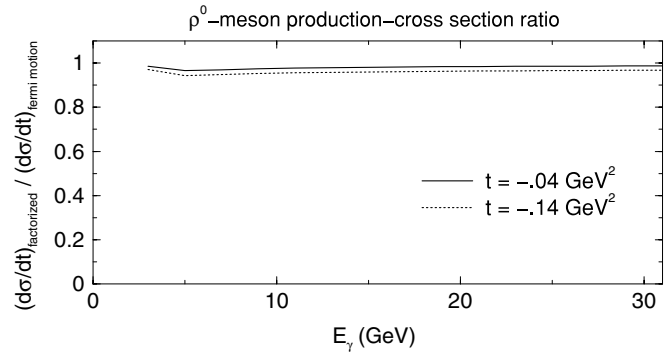


FIG. 9. The energy dependence of the ratio between the differential cross section calculated with the usual factorization assumption and the differential cross section calculated with factorization breakdown taken into account.

a kinematic region in which no known multiple-scattering formalism works. Numerically, our calculation is correct only in the region of  $-t$  above the dip at small  $-t$ ; that is, when  $-\hat{t} + \hat{t}_{\min}$  is greater than a few tens of mega-electron-volts.

Next we plot consider the total unpolarized cross sections as functions of photon energy for a set of fixed values of  $-t$ . This allows us to compare the factorized and unfactorized calculations directly and to determine at approximately what value of energy the transition to the VMD-Glauber regime occurs. Recall that it is the motion of the nucleons in the deuteron (the Fermi motion) that leads to the nonfactorizability of the basic amplitudes. Factorization refers the practice of ignoring the dependence of nucleon momentum inside the basic amplitudes when integrals over nucleon momentum are performed. The use of nonfactorized amplitudes is the essential difference between our approach and the usual Glauber approach. The ratio of the cross section with the usual factorization assumption to the cross section that accounts for nonfactorizability effects (Fermi motion) is shown in Fig. 9. The upper panel refers to the case of  $\rho^0$  production, whereas the lower panel refers to  $\phi$  production. The ratio is given for two small values of  $-t$ :  $t = -0.04$  GeV<sup>2</sup> and  $t = -0.14$  GeV<sup>2</sup>.

The upper panel demonstrates that the effect of nonfactorizability is small for the case of  $\rho^0$  for the entire range of intermediate energies. This is in sharp contrast to the case of  $\phi$  production in the lower panel of Fig. 9. Note that we plot only the case of  $t = -0.04$  GeV<sup>2</sup> down to  $E_\gamma = 5$  GeV for the  $\phi$ -meson case. This is because, for photon energies lower than 5 GeV,  $t = -0.04$  GeV<sup>2</sup> becomes too close to  $t_{\min}$ .

On the other hand, for the curve corresponding to  $t = -0.14$  GeV, there is nearly a 30% suppression of the factorized cross section relative to the unfactorized cross section at the lowest energy,  $E_\gamma = 3$  GeV, shown in the lower panel of Fig. 9. We emphasize that this result is for a photon energy (3 GeV) that is well into the kinematic region where the eikonal approximation may be applied (see Sec. II A) and that  $-t = 0.14$  GeV<sup>2</sup> is certainly large enough relative to  $-t_{\min} = 0.036$  GeV<sup>2</sup> that there are none of the problems discussed earlier related to nearness to  $-t_{\min}$ . Therefore our method of calculation is ideally suited to the kinematics of the dotted curve in Fig. 9, where a significant effect from the breakdown of the factorizability assumption is already seen.

Note from the general behavior in Fig. 9 that the cross section rises when the factorization assumption is removed. This effect is mainly due to the suppression of multiple scattering when nonfactorizability is taken into account. To see this, note that at  $-t = 0.14$  GeV<sup>2</sup> the main effect of double scattering in the usual Glauber approach is to produce a large negative cross term that has a canceling effect. All terms apart from the Born term and the interference term are negligible at this value of  $t$ . (See, for example, the upper left-hand panels of Figs. 5 and 6.) Therefore, if multiple scattering is suppressed, as it is in our approach, then the absolute value of the cross term becomes smaller, and the Born contribution is no longer suppressed by multiple scattering. Thus the curve representing our approach in Fig. 9 is smaller than what is found in the standard Glauber calculation.

At high energies we expect the two methods to agree, and they do within the range of experimental uncertainties of nonrelativistic deuteron form factors. The fact that the two methods have slight disagreement at high energies is a reflection of the fact that, even at high energies, we have not calculated the form factor with exactly the same approximation as in the usual Glauber approach. In the usual nonrelativistic form factor, any dependence on longitudinal transferred momentum is ignored. If one takes into account exact kinematics, one finds that there are two distinct effects that may cause this assumption to be violated. It is easiest to see this by writing out the exact expression for the transferred longitudinal momentum:

$$l_z = -\frac{t}{2M_D} + \frac{M_V^2 - t}{2E_\gamma}. \quad (34)$$

From this we see that there are two approximations that are normally made in the Glauber approach that allow us to neglect  $l_z$ . The first is the ultrarelativistic approximation for the incident vector meson,  $E_\gamma \gg M_V$ , and the second is the nonrelativistic approximation for the exchanged four-momentum,  $-t \ll M_D$ . If  $t$  is small relative to  $M_D$  then there is still a significant contribution to  $l_z$  when  $M_V$  is nonnegligible relative to  $E_\gamma$ . This is the effect that interests us in this paper. It is safe to use the nonrelativistic form factor because the transferred energy is

$$l_0 = -\frac{t}{2M_D}, \quad (35)$$

which is small at small  $-t$ . On the other hand, as long as  $t$  is not exactly zero, there will be a component of  $l_z$  that does not die

out with energy. This effect represents the error induced when relativistic recoil is ignored. In the future we plan to generalize the formalism to the case of light-cone wave functions so that it may be extended to higher  $-t$ .

## V. DIRECTIONS FOR FUTURE WORK

### A. Extraction of basic amplitudes

We emphasize that the work in this paper is a first step in refinements to the usual techniques applied to multiple scattering in vector meson production from the deuteron. We plan to extend these refinements in the future to include, for example, light-cone kinematics in the treatment of the deuteron wave function and spin-flip effects. Obtaining precise parametrizations of the  $s$  and  $t$  dependences is one of several steps needed for refinements in the calculation. We note that a peak in the energy dependence has been reported in Ref. [16] for photoproduction of  $\phi$  mesons from a proton target at  $E_\gamma = 2$  GeV, and it is these data that we used in our parametrization (see Appendix A). We would like to point out, however, that the measurements in Ref. [16] are for the differential cross section at  $t = t_{\min}$ . Therefore, since the value of  $t_{\min}$  varies significantly with energy in these near-threshold measurements, then the reported measurements give the differential cross section at very different values of  $t$ . We have indicated this in Fig. 10(A). To infer the energy dependence at a *fixed* value of  $t$ , one needs to assume a form for the  $t$  dependence. The actual  $t$  dependence at these low energies is not well known, but it is straightforward to see that even a simple exponential  $t$  dependence will have an effect on the shape of the overall energy dependence of the cross section. As an example, we have plotted in Fig. 10(A) the data as they were originally presented in Ref. [16] alongside Fig. 10(B) in which the data have been shifted to a fixed value of  $t$ . We have used an exponential slope parameter of 4 GeV<sup>2</sup> which gives reasonable agreement with the data. In the original form of the plot, Fig. 10(A), the data are shown at a different value of  $t$  at each energy. The highest value of  $-t_{\min}$  occurs at the lowest energy plotted, which is around 1.6 GeV. In Fig. 10(B) we have replotted the energy dependence, but with the value of  $t$  for each data point fixed at  $-t_{\min}$  for  $E_\gamma = 1.6$  GeV since this is the largest value of  $-t$  that is kinematically allowed for every point on the plot. Let  $t_{\min}[1.6]$  represent the value of  $-t_{\min}$  at  $E_\gamma = 1.6$  GeV. Then,

$$\left. \frac{d\sigma}{dt} \right|_{t=t_{\min}[1.6]} = \left. \frac{d\sigma}{dt} \right|_{t=t_{\min}} e^{4.0 \text{ GeV}^{-2}(t_{\min}[1.6]-t_{\min})}. \quad (36)$$

We use this to obtain Fig. 10(B). We see that much of the peaklike behavior is removed. Without a fuller understanding of the  $t$  dependence, therefore, it cannot be ruled out that the observed peak arises from purely kinematical effects. However, the fact that the cross section at fixed  $t$  does increase at smaller  $E_\gamma$  is evidence that OZI-violating meson exchange effects become important at these energies.

Recently, preliminary data were reported from SPring-8/LEPS [24] that measured the dependence of the  $\phi$ -meson production cross section at  $E_\gamma \sim 2$  GeV on the linear polarization of the photon. Significant polarization is observed that requires the presence of a nonvacuum exchange like  $\pi$ ,  $\eta$

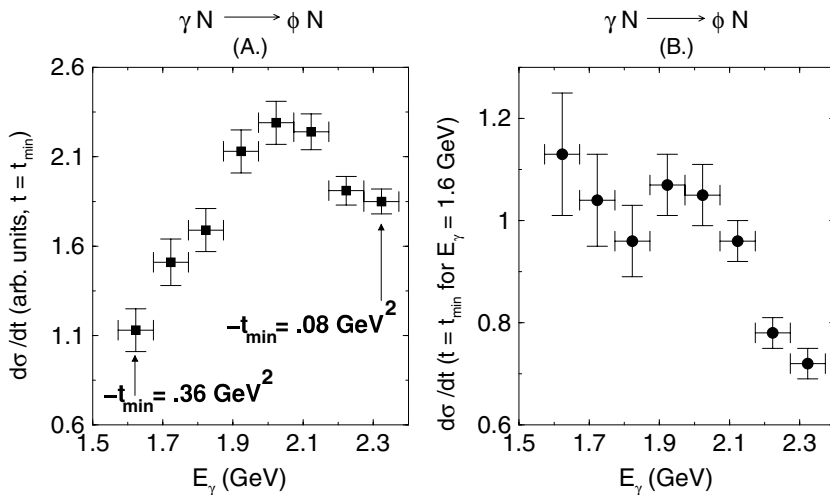


FIG. 10. Plot of recent data from LEPS, taken from Ref. [16]. We indicate the significant variation of  $t_{\min}$  with photon energy. This may have an effect on the overall energy dependence of the cross section. (A) shows how the data were originally presented: at a different value of  $t$  for each energy. In (B) we shifted all of the data points to the same value of  $t$  by assuming a constant slope parameter of  $4 \text{ GeV}^{-2}$ . Each point in (B) corresponds to the differential cross section at the fixed value of  $t$  corresponding to  $t_{\min}$  for a 1.6-GeV photon. Note the different scales on the axes in (B).

exchange. Such exchanges lead to spin flip in the nucleon vertex. These contributions for small  $t$  are strongly suppressed for coherent production off the deuteron (pion exchange does not contribute in any case because of the zero isospin of the deuteron). These effects are determined by the deuteron magnetic form factor, which is much smaller than the electric form factor. Hence the coherent production of the  $\phi$ -meson may be used as a spin analyzer of the elementary amplitude in the kinematics in which double scattering is a small correction. This topic has already been discussed in Ref. [7]. In the spirit of the original Glauber approach, we neglected spin effects in this paper for the sake of simplicity. Future work will involve generalizations of our method to the case of spin-dependent basic amplitudes. However, if one fits a combination of Pomeron trajectory and Reggeon trajectory to the recent preliminary SPring-8/LEPS data and then extrapolates to 3 GeV, then it appears that less than 20% of the basic  $\gamma D$  cross section is due to spin flip, whereas the corrections found in this paper that are due to nonfactorizability are as large as 30% at 3 GeV [24].

Before ending our analysis, we mention that, because  $VN$  cross sections are extracted from the multiple-scattering term, quantities sensitive to the deuteron polarization would be ideal for testing whether the  $VN$  cross section is unusually large. To emphasize this, the cross section for scattering from a polarized deuteron, from  $m = +/ - 1$  to  $m = +/ - 1$ , is plotted in Fig. 11 where the result of using a typical value for the total  $\phi N$  cross section (11 mb) is compared with the case in which the  $\phi N$  cross section is enhanced by a factor of 3. (For clarity we have plotted only the sum of all the terms from the squared amplitude rather than each term separately.) The sharp dip that normally appears is due to the sharp dip in the Born cross section. However, the double-scattering cross section is nearly flat in  $-t$ . Therefore in the summed cross section the double scattering term dominates in the region of the dip and may even cause the dip to vanish entirely if it becomes very large. Figure 11 shows that, even with the suppression of the double-scattering term that results from the nonfactorizability that we have been discussing, the dip in the cross section is observed to flatten out when the basic  $\phi N$  cross section is abnormally large.

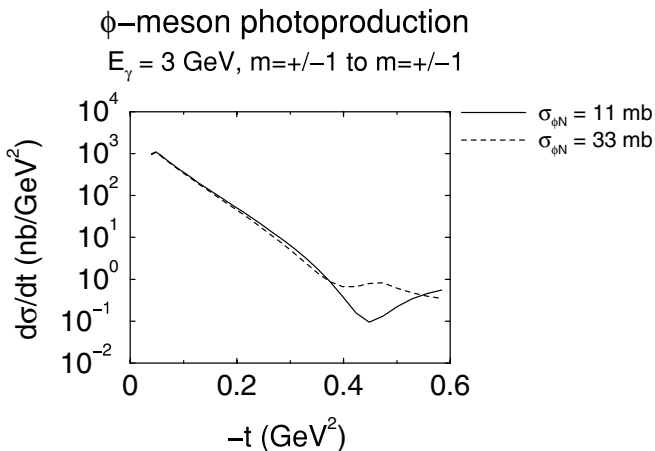


FIG. 11. The energy dependence of the  $m = +/ - 1$  to  $m = +/ - 1$  differential cross section for  $\phi$ -meson photoproduction with  $E_\gamma = 3 \text{ GeV}$ . The dashed curve shows the result of increasing the typical basic  $\phi N$  cross section by a factor of 3.

### B. The problem of bound-state amplitudes

We have treated the struck nucleon as being on-shell, which is consistent with the neglect of terms quadratic in nucleon momentum. However, *immediately* at the threshold for particle production, the  $\gamma N \rightarrow VN$  amplitude has very unpredictable behavior, which may be modified significantly when the nucleon is in a bound state. This is especially clear when we realize that, for a given photon energy,  $-t_{\min}$  is different for a deuteron and an on-shell nucleon target. We cannot predict the effects of the off-shellness of the bound nucleon without a complete, relativistic understanding of the basic amplitude. However, we have made predictions in the region of kinematics where it is reasonable to assume that the bound-state amplitude is the same as that of the free-nucleon amplitude. If one includes dependence on the nucleon virtuality in the basic amplitude, then one may write the amplitude as  $\hat{F}(\hat{s}, \hat{t}, k_N^2)$ . For  $k_N^2 = m_N^2$ , the amplitude reduces to the free-nucleon amplitude. As we have stated,  $k_N^2 = m_N^2$  up to corrections of the order of  $\mathbf{k}_N^2/m_N^2$  or higher, whereas  $\hat{s}$  has linear-order

corrections in nucleon momentum. Thus, if  $\hat{F}(\hat{s}, \hat{t}, k_N^2)$  is an analytic function of kinematic variables, then there will be linear-order corrections in nucleon momentum that are due to  $\hat{s}$  whereas the lowest-order corrections that are due to the virtuality of the bound nucleon are of only quadratic order in nucleon momentum. In other words, Fermi motion effects may be important even when it is appropriate to neglect the off-shellness of the bound-state amplitude. Of course, all of this depends on the validity of using  $\mathbf{k}_N/m_N$  as a small expansion parameter that is true only if the basic amplitude has relatively weak  $s$  dependence. This is one reason why we emphasize that we are considering intermediate energies rather than low energies. One may also include the deuteron binding energy in the calculation of the mass of the bound nucleons, but the binding energy arises from the full consideration of relativistic binding and higher-order terms in nucleon momentum, so considering the nucleon binding energy is not consistent with the neglect of higher-order nucleon momentum terms or the use of a nonrelativistic potential for the  $NN$  interaction.

In this subsection we propose a rough a way to test the validity of the on-shell amplitude approximation. We do this in the next few paragraphs by directly comparing the amplitude when it is evaluated at the value of  $t_{\min}$  for the deuteron with the case in which it is evaluated at  $t_{\min}$  for a free nucleon with  $s$  given by the exact expression for  $\hat{s}$ :

$$\hat{s} = 2E_\gamma \left( M_D - \sqrt{m_N^2 + \mathbf{k}^2} + k_z \right) + \left( M_D - \sqrt{m_N^2 + \mathbf{k}^2} \right)^2 - \mathbf{k}^2. \quad (37)$$

The value of the nucleon three-momentum thus parametrizes the off-shellness of the bound nucleons.  $t'_{\min}$  denotes the lower bound of  $-t$  for the free nucleon, whereas  $t_{\min}$  is the lower bound of  $-t$  for the deuteron. The struck nucleon inside the deuteron for the unprimed case has  $\hat{s}$  given by Eq. (37). We now consider the case of a free nucleon, with the same  $\hat{s}$  as for the bound nucleon, but with the nucleon on-shell (i.e.,  $k^2 = m_N^2$ ) and with a fixed value for  $k_z$ . So that the free-nucleon energy corresponds to the bound nucleon energy, we continue to use  $M_D - \sqrt{m_N^2 + \mathbf{k}^2}$  for the energy of the struck nucleon. In short, we are comparing  $t_{\min}$  for  $\gamma$  scattering off a deuteron at rest with  $t'_{\min}$  for  $\gamma$  scattering off a free nucleon, with energy corresponding to that of the bound nucleon in both cases.

We expect the rate of variation of the basic amplitude with  $t$  to be very large near  $t_{\min}$ . If there is a significant contribution to the integral in Eq. (5) from regions near  $t_{\min}$ , then  $t_{\min}$  should nearly equal  $t'_{\min}$  in order to make the on-shell amplitude a valid approximation to the bound-state amplitude. We can use the difference between these two values of  $t_{\min}$  to estimate the effect of the off-shellness on the the amplitude.

To test the effect of the off-shellness of the basic amplitude, we may consider two extremes. First, the bound-state basic amplitude could be evaluated at the physical value of  $t$  for the photon-deuteron process. That is, we could calculate the amplitude  $\hat{F}(\hat{s}, t)$  at  $t$ , where  $t$  is the physical value of  $t$  for the photon-deuteron process. In this case, since  $t_{\min}$  is smaller for the deuteron than  $t'_{\min}$  is for the nucleon, then we are probably overestimating the cross section. On the other

hand, we could evaluate the basic amplitude at  $F[\hat{s}, t - (t_{\min} - t'_{\min})] = F(\hat{s}, t - \Delta t)$ , where  $t'_{\min}$  is the minimum  $t$  for the free, on-shell nucleon. With this second method for choosing which value of  $t$  to use in the basic amplitude, the basic amplitude behaves as the free, on-shell nucleon amplitude in the region of  $t$  close to  $t_{\min}$ . Hence, with this method, we are probably underestimating the value of the basic amplitude. In the high-energy limit,  $\Delta t$  vanishes and the two amplitudes are equal, and the difference between the two provides an estimate of the off-shell effects. (Note that we must specify a value for  $\mathbf{k}$  in order to make a comparison.) Any amplitude that has a relatively slow and smooth variation with  $t$  will yield a small difference between  $\hat{F}(\hat{s}, t)$  and  $F(\hat{s}, t - \Delta t)$ . We made this comparison for  $\phi$ -meson production with the parametrization in Appendix A, and we find only a few percent deviation. We conclude that at a few giga-electron-volts above threshold it is reasonable to continue using the on-shell amplitude of the nucleon.

## VI. SUMMARY AND CONCLUSIONS

The main conclusion of this paper is that the effect of factorization breakdown is significant for intermediate photon energies. The Glauber approach is, strictly, applicable only for the case of very high photon energies. However, there are current attempts to apply the factorization assumption of Glauber theory to the  $\phi$ -meson production reaction at energies as low as 1.5 GeV in both experimental and theoretical research. Therefore, to salvage the situation in the energy range of a few giga-electron-volts above threshold, we have outlined steps one must follow in order to obtain corrections to leading order in the bound nucleon momentum and transferred momentum. The main steps are essentially those of the original diagrammatic formulation of Glauber theory in terms of momentum space integrals and its extension to vector meson production [10–12]; we have started with most of the original assumptions, but we have removed the assumptions of factorizability, ultrarelativistic kinematics, or VMD for the basic amplitudes, and we have numerically evaluated all integrals directly without any factorization approximations. By using a simple model for the basic amplitude (we restore VMD for the simple model) based on a fit to old and recent data, we have shown that, away from  $t = t_{\min}$ , ignoring Fermi motion (and the resulting breakdown of factorizability) can lead to a significant error in basic cross-sections extracted from  $\gamma D \rightarrow \phi D$  cross-section data (see Fig. 9). This effect will certainly need to be taken into account in future searches for new production mechanisms at intermediate energies. The breakdown in factorizability arises as a consequence of both the nonnegligible longitudinal momentum exchanged and the nonnegligible Fermi motion. An important point is that a key source of the departure from factorizability is the inadequacy of assuming the nearly flat  $s$  dependence predicted by Regge theory in the basic amplitudes. Therefore models of the basic  $\gamma N \rightarrow VN$  amplitude or the  $VN \rightarrow VN$  amplitude that depart significantly from nearly flat  $s$  dependence must include *at least* the linear-order nucleon momentum corrections of this paper if they are to be used in calculations with a deuteron target. This correction arises purely from the fact that the bound nucleons have nonvanishing momentum, and it must

be included regardless of the details of a particular model of the basic amplitudes. For the case of  $\phi$ -meson production, we find that our approach is reasonable when we use our particular simple model of the basic amplitude and as long as the photon energy is around 3 GeV or higher and  $t$  is not too close to  $t_{\min}$ .

However, we stress that in a model of the basic  $\gamma N \rightarrow VN$  amplitude that predicts much wilder energy dependence at intermediate energies than what we have assumed, the linear-order corrections will not be sufficient, and a complete and precise understanding of the  $NN$  interaction and the bound-state nucleon amplitudes are necessary to make a correct calculation. For the  $\phi$ -meson photoproduction cross section ( $M_\phi \approx 1.02$  GeV), the amplitude may vary wildly with energy at  $E_\gamma = 2$  GeV or lower because of the very close proximity to threshold. For this reason, and because the eikonal approximation begins to break down, basic cross sections for photoproduction from the nucleon extracted from data for photoproduction from the deuteron are suspect for photon energies less than or equal to 2 GeV for the  $\phi$  production reaction.

In our sample calculation, we observe that the contribution from double scattering becomes numerically suppressed relative to the Born approximation as the incident photon energy decreases. However, the multiple-scattering terms are what lead to the characteristic  $A$  dependence of the Glauber theory for complex nuclei,  $\sigma_{\text{tot}} \sim A^{2/3}$ . This suggests that an extension of our methods to complex nuclei will yield a rather different  $A$  dependence for the cross section at intermediate energies from what is predicted at high energies. Hence there will need to be a revision in efforts to extract basic cross sections from nuclear data by use of extrapolations in  $A$ . The extension to complex nuclei, however, requires much more work. We note, however, that data given in Ref. [25] were interpreted as implying a very high  $\phi N$  total cross section on the basis of a very traditional Glauber approach at energies of only a few giga-electron-volts. Therefore our next step will be to determine how the nonfactorization effects discussed in this paper affect a general, incoherent Glauber series. Furthermore, since it is apparent that spin effects will be important, then a generalization with spin-dependent amplitudes will be needed.

We purposely oversimplified our analysis here for the purposes of demonstration. In particular, we applied the VMD hypothesis at energies at which it is suspect and we neglected fluctuations and  $\omega - \phi$  mixing in the intermediate vector meson in the double-scattering term. Further analysis will need to include these effects. To make further numerical progress, we will need firmer parametrizations of the basic cross sections for vector meson production from nucleons. For theoretical work, it would be useful for the purposes of comparison to have a widely agreed-on set of parametrizations. We also need to consider the calculation in light cone coordinates and the effects of spin flip. We will pursue these issues in future work.

Finally, we need a complete understanding of the off-shell amplitudes if we are to take into account the higher-order momentum corrections that will be necessary just at the threshold, though we have argued that for smoothly varying basic cross sections, the effect of off-shellness in the amplitudes is small relative to the effect of linear-order corrections in nucleon momentum.

## ACKNOWLEDGMENTS

T.C. Rogers thanks Steve Heppelmann and David Landy for useful discussions and Isaac Mognet and Nick Conklin for sharing computer facilities. This work is supported by U.S. Department of Energy grants under contracts DE-FG02-01ER-41172 and DE-FG02-93ER40771.

## APPENDIX A: PARAMETRIZATIONS

Here we describe the fits of the basic cross sections that we used for our sample calculations. The object here is not necessarily to produce very accurate parametrizations, but rather to devise parametrizations that demonstrate the effects of Glauber factorization while being consistent with recent and established experimental results.

First we consider the  $\gamma N \rightarrow \rho^0 N$  differential cross section. For this we use a simple exponential  $t$  dependence with a typical exponential slope of  $B = 7.0$  GeV $^{-2}$  and an overall normalization of  $105 \mu\text{b}/\text{GeV}^2$ . (See, e.g., Ref. [1].) It is known that at low energies the normalization undergoes a steep rise. We take this into account in our calculation by including a factor of  $(1 + \frac{a}{E_\gamma^4})$  in the overall normalization and then doing a least-squares fit to obtain the parameter  $a$ . We find that  $a \approx 32.7$ . The cross section is thus

$$\frac{d\sigma}{dt} = 105 \frac{\mu\text{b}}{\text{GeV}^2} \left( 1 + \frac{32.7 \text{ GeV}}{E_\gamma^4} \right) e^{7.0 \text{ GeV}^{-2} t}. \quad (\text{A1})$$

The result is shown in Fig. 12. As is seen in the main part of the text, the variation is too weak to introduce a very large effect on the final  $\gamma D \rightarrow \rho^0 D$  cross section from Fermi motion.

The case of the  $\phi$  meson is more complicated because of the irregular behavior near threshold. The main point is to interpolate smoothly between recent low-energy data and the standard higher-energy parametrization. The normalization of the low-energy data, taken from recent experimental work in Ref. [16], is obtained from an effective Pomeron and pseudoscalar exchange model [26], as was presented in Ref. [16]. We continue to use this so that our model will

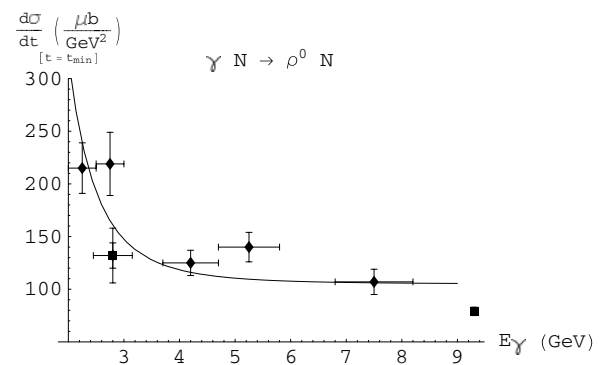


FIG. 12. We obtain this fit by using data from Refs. [27–29] (listed in Ref. [1]). We use an inverse-fourth function at low energies and apply a least-squares fit. The peak in the parametrization yields a small effect from Fermi motion (at a few giga-electron-volts) because of the small mass of the  $\rho^0$ .

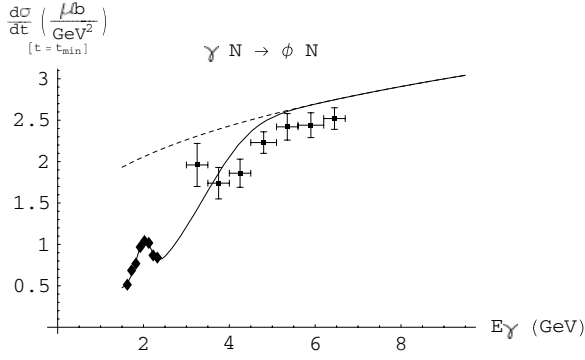


FIG. 13. The low-energy data here are from Ref. [16]. The curve at high energies was taken from Ref. [1]. The dashed curve shows its extension to lower energies. The high-energy data are taken from Ref. [30] and are presented to establish the consistency of the high-energy parametrization. The curve at low energies was fit to the low-energy data of Ref. [16] by use of a least-squares fit.

be consistent with current work. Bauer *et al.* obtained the high-energy parametrization in Ref. [1] by fitting a diffraction-like cross section to a large set of experimental data. We want to interpolate quickly but smoothly between the low-energy and high-energy data. There is an exponential factor  $e^{Bt}$  associated with both the high- and the low-energy behavior, but the slope  $B$  is around  $3.4 \text{ GeV}^{-2}$  for the low-energy behavior ( $E_\gamma \lesssim 4.0 \text{ GeV}$ ) while it is around  $4.8 \text{ GeV}^{-2}$  for the high-energy behavior. Thus for the exponential slope we use

$$B(E_\gamma) = [4.8 - (4.8 - 3.4)e^{-0.001 \text{ GeV}^{-4} E_\gamma^4}] \text{ GeV}^{-2}. \quad (\text{A2})$$

Next, for the low-energy region, there is no Regge slope. That is,  $\alpha' = 0$  in the factor  $s^{\alpha't}$ . However, in the high-energy region,  $\alpha' = 0.27 \text{ GeV}^{-2}$ . Thus we use

$$\alpha'(E_\gamma) = 0.27(1 - e^{-0.001 \text{ GeV}^{-4} E_\gamma^4}) \text{ GeV}^{-2}. \quad (\text{A3})$$

Now we consider the behavior of  $\frac{d\sigma}{dt}|_{t=0}$  for photoproduction of the  $\phi$  meson from a proton target. The high-energy parametrization in Ref. [1] is

$$\left. \frac{d\sigma}{dt} \right|_{t=0} = 1.34s^{0.28}, \quad (\text{A4})$$

and, as in Ref. [1], overall units will be understood to be  $\mu\text{b}/\text{GeV}^2$ . To match to the data of Ref. [16] we want a peak to appear at around  $E_\gamma = 2.0 \text{ GeV}$ . Therefore we adjust the parametrization to

$$\left. \frac{d\sigma}{dt} \right|_{t=0} = 1.34s^{0.28}[1 + ae^{-b(E_\gamma - c)^2}]. \quad (\text{A5})$$

We use Eq. (A5) to fit to the low-energy data of Ref. [16] while ensuring that the high-energy parametrization of Eq. (A4) is reproduced at high energies. We find  $a = 0.71$ ,  $b = 16.5 \text{ GeV}^{-2}$ , and  $c = 2 \text{ GeV}^{-2}$ . Finally, we note that the low-energy data are actually given for  $t = t_{\min}$  rather than  $t = 0$ . Therefore we must be sure to include a factor of  $e^{B(E_\gamma)t_{\min}}$  in the final result for  $\frac{d\sigma}{dt}|_{t=0}$ . The result of our parametrization for  $\frac{d\sigma}{dt}|_{t=0}$  for the  $\phi$  meson is shown in Fig. 13. We point out

that, in the intermediate-energy range at around  $E_\gamma = 3 \text{ GeV}$ , the energy dependence is not completely flat, but is smooth and slow enough that its effect may be treated as a small correction.

## APPENDIX B: DEUTERON POLARIZATION

In this appendix, we give an overview of the treatment of deuteron spin as it is presented in [21]. To evaluate the cross section, we must determine how the operator  $\tilde{\Psi}_m^\dagger(\mathbf{k} - \frac{1}{2})\tilde{\Psi}_m(\mathbf{k})$  acts on the spin-1 ground state of the deuteron. The nonrelativistic deuteron wave function in momentum space is written in terms of  $S$  and  $D$  states by means of the formula

$$\tilde{\Psi}_m(\mathbf{k}) = [\tilde{u}(k) - 8^{-1/2}\tilde{w}(k)\hat{S}_{12}]|\hat{q}, m\rangle, \quad (\text{B1})$$

where

$$\begin{aligned} \tilde{u}(k) &\equiv \frac{1}{\sqrt{2\pi}} \int_0^\infty r dr j_0(kr)u(r), \\ \tilde{w}(k) &\equiv \frac{1}{\sqrt{2\pi}} \int_0^\infty r dr j_2(kr)w(r). \end{aligned} \quad (\text{B2})$$

The real functions,  $u(r)$  and  $w(r)$ , are taken from any realistic model of the deuteron wave function, and in our computations we use the Paris potential [22]. The functions  $j_0$  and  $j_2$  are the zeroth- and second-order spherical Bessel functions. In Eq. (B1),  $|\hat{q}, m\rangle$  is a spin-1 spinor representing the total angular momentum of the deuteron and  $\hat{q}$  is the quantization axis. The tensor operator  $\hat{S}_{12}$  acts on the total angular-momentum state to produce a sum over total spin states. In terms of the spins of the nucleons, it is given by

$$\hat{S}_{12} = \frac{3(\sigma_1 \cdot \mathbf{r})(\sigma_2 \cdot \mathbf{r}) - \sigma_1 \cdot \sigma_2}{r^2}. \quad (\text{B3})$$

The projection onto total spin states is

$$\begin{aligned} \hat{S}|0, \hat{q}\rangle &= \sqrt{\frac{48\pi}{5}}Y_2^1(\theta, \phi)|-1\rangle \\ &\quad - \sqrt{\frac{64\pi}{5}}Y_2^0(\theta, \phi)|0\rangle + \sqrt{\frac{48\pi}{5}}Y_2^{-1}(\theta, \phi)|1\rangle \\ \hat{S}|-1, \hat{q}\rangle &= \sqrt{\frac{16\pi}{5}}Y_2^0(\theta, \phi)|-1\rangle \\ &\quad - \sqrt{\frac{48\pi}{5}}Y_2^{-1}(\theta, \phi)|0\rangle + \sqrt{\frac{96\pi}{5}}Y_2^{-2}(\theta, \phi)|1\rangle \\ \hat{S}|1, \hat{q}\rangle &= \sqrt{\frac{96\pi}{5}}Y_2^2(\theta, \phi)|-1\rangle \\ &\quad - \sqrt{\frac{48\pi}{5}}Y_2^1(\theta, \phi)|0\rangle + \sqrt{\frac{16\pi}{5}}Y_2^0(\theta, \phi)|1\rangle. \end{aligned}$$

The functions  $Y$  are the usual spherical harmonic functions. With these equations, we can calculate the effective form factor for each polarization and then sum and average over final/initial deuteron polarizations.

- [1] T. H. Bauer, R. D. Spital, D. R. Yennie, and F. M. Pipkin, *Rev. Mod. Phys.* **50**, 261 (1978) [Erratum-*ibid.* **51**, 407 (1979)].
- [2] R. P. Feynman, *Photon-Hadron Interactions* (Addison-Wesley Longman, Reading, Massachusetts, 1972).
- [3] V. Franco and R. J. Glauber, *Phys. Rev.* **142**, 1195 (1966).
- [4] R. L. Anderson *et al.*, *Phys. Rev. D* **4**, 3245 (1971); I. D. Overman, Ph.D. thesis, SLAC-140, UC-34, Stanford University, 1971.
- [5] L. Frankfurt, G. Piller, M. Sargsian, and M. Strikman, *Eur. Phys. J. A* **2**, 301 (1998); L. Frankfurt, W. Koepf, J. Mutzbauer, G. Piller, M. Sargsian, and M. Strikman, *Nucl. Phys.* **A622**, 511 (1997).
- [6] A. I. Titov, T. S. H. Lee, H. Toki, and O. Streltsova, *Phys. Rev. C* **60**, 035205 (1999).
- [7] A. I. Titov, M. Fujiwara, and T. S. H. Lee, *Phys. Rev. C* **66**, 022202(R) (2002).
- [8] Y. S. Oh, *J. Korean Phys. Soc.* **43**, S20 (2003).
- [9] L. L. Frankfurt and M. I. Strikman, *Nucl. Phys.* **B250**, 143 (1985).
- [10] K. S. Kolbig and B. Margolis, *Nucl. Phys.* **B6**, 85 (1968).
- [11] V. N. Gribov, *Sov. Phys. JETP* **29**, 483 (1969) [*Zh. Eksp. Teor. Fiz.* **56**, 892 (1969)].
- [12] L. Bertocchi, *Nuovo Cimento A* **11**, 45 (1972).
- [13] L. L. Frankfurt, W. R. Greenberg, G. A. Miller, M. M. Sargsian, and M. I. Strikman, *Z. Phys. A* **352**, 97 (1995).
- [14] L. L. Frankfurt, M. M. Sargsian, and M. I. Strikman, *Phys. Rev. C* **56**, 1124 (1997); M. M. Sargsian, *Int. J. Mod. Phys. E* **10**, 405 (2001).
- [15] S. Jeschonnek, *Phys. Rev. C* **63**, 034609 (2001).
- [16] T. Mibe *et al.* (LEPS Collaboration), *Phys. Rev. Lett.* **95**, 182001 (2005).
- [17] G. D. Alkhozov, S. L. Belostotsky, and A. A. Vorobev, *Phys. Rep.* **42**, 89 (1978).
- [18] K. Garrow *et al.*, *Phys. Rev. C* **66**, 044613 (2002).
- [19] D. Binosi and L. Theussl, *Comput. Phys. Commun.* **161**, 76 (2004).
- [20] G. E. Brown and A. D. Jackson, *The Nucleon-Nucleon Interaction* (North-Holland, Amsterdam, 1976).
- [21] V. Franco and R. J. Glauber, *Phys. Rev. Lett.* **22**, 370 (1969).
- [22] M. Lacombe, B. Loiseau, J. M. Richard, R. Vinh Mau, J. Cote, P. Pires, and R. de Tournell, *Phys. Rev. C* **21**, 861 (1980).
- [23] H. Alvensleben *et al.*, *Phys. Rev. Lett.* **27**, 444 (1971).
- [24] Talk given by Keito HOREI, "Measurement of photoproduction of  $\phi$ -mesons near threshold by SPring-8/LEPS," 27 October 2005, at the Particles and Nuclei International Conference in Santa Fe, NM, 24–28 October 2005, to appear in the proceedings of PANIC05; <http://panic05.lanl.gov/>
- [25] T. Ishikawa *et al.*, *Phys. Lett.* **B608**, 215 (2005).
- [26] A. I. Titov and T. S. H. Lee, *Phys. Rev. C* **67**, 065205 (2003).
- [27] J. Ballam *et al.*, *Phys. Rev. D* **5**, 15 (1972).
- [28] Y. Eisenberg, B. Haber, E. Kogan, E. E. Ronat, A. Shapira, and G. Yekutieli, *Nucl. Phys.* **B42**, 349 (1972).
- [29] J. Ballam *et al.*, *Phys. Rev. D* **7**, 3150 (1973).
- [30] H. J. Behrend *et al.*, *Nucl. Phys.* **B144**, 22 (1978).